| Sl. No. | **IIT Ropar**<br>**List of Recent Publications with Abstract**<br>**Coverage: February, 2020** |
|---|---|
| 1. | A Differential Evolution-Based Inverse Method to Optimize Blade Configurations in Elliptical-Bladed Savonius Wind Turbines<br>N Alom, R Das, UK Saha - ASME 2019 Gas Turbine India Conference, 2020<br><br>**Abstract:** It is well-known that elliptical-bladed Savonius wind turbine yields relatively better performance than conventionally used semicircular-bladed turbines. This is mainly due to lesser tip loss and delayed flow separation that allow the elliptical turbine to acquire higher rotational speeds than semicircular turbine under a given wind load. In this work, an experimentally-validated inverse analysis is done to determine the optimum blade configurations involving the chord length, turbine height, aspect ratio, and the necessary overlap ratio to derive a required power and torque from elliptical-bladed Savonius wind turbines. Due to obvious advantages of evolutionary metaheuristic optimizers in general, here differential evolution (DE) search algorithm is used to solve the inverse problem through a least-squares minimization of the relevant objective function. The objective function is further subjected to feasible bounds of the unknown design variables. The effects of blockage corrections are duly considered and the variations of the design variables along with the objective function are studied over a range of iterations of the DE algorithm. Through comprehensive analysis, it is highlighted from the present study that for harvesting a given performance, rotor swept area can be reduced by 6.25% with respect to the available experimental data under identical operating conditions of the wind turbine. Multiple blade configurations can be acquired, all of which invariably satisfy the required performance criterion. This study also highlights that amongst various dimensional parameters, turbine height and aspect ratio play more prominent role than chord length and overlap ratio and the blade chord influences only the torque but not markedly the power. The results obtained from the present work are proposed to facilitate the concerned designer to explore various feasible blade designs and determine the suitable one, thereby avoiding valuable time elapsed in repetitive fabrication and testing of various designs. |
| 2. | A Fog based Building Fire Evacuation Framework<br>A Kaur, N Auluck - Proceedings of the Australasian Computer Science Week Multiconference, 2020<br><br>**Abstract:** Fog Computing extends traditional cloud based services to the edge of the network, close to where the data is generated. This technology fills a performance void in the cloud-to-thing architecture. By leveraging Fog Computing, the computation, storage, communication and decision making can be carried out by fog nodes. Due to significant latency, the cloud is not the best option for emergency response services, such as fire-fighting. For efficient fire-fighting, decisions should be made accurately and rapidly. In this paper, we propose an algorithm called FAFCA (Fog Assisted Fire Control Algorithm). In the wake of a fire in a building , this algorithm efficiently routes the evacuees to the shortest and least congested exits in a short span of time. The crux of the algorithm is that due to the lower communication delay between the fog nodes and the evacuees, data processing is done faster, which results in making evacuation decisions rapidly. The best path for the evacuees present in the building is calculated by the algorithm after taking various parameters into account, such as exit capacity, distance to exits and distribution of evacuees. Simulation results show that our proposed algorithm FAFCA |

| | |
|---|---|
| | decreases the latency as well as cost significantly, when compared to a cloud based algorithm and a random path selection algorithm. |
| 3. | **A Revisit to the Infection Source Identification Problem under Classical Graph Centrality Measures**<br>SS Ali, T Anwar, SAM Rizvi - Online Social Networks and Media, 2020<br><br>**Abstract:** The high connectivity of the modern day world has lead to the easy diffusion of harmful information content like rumors, computer viruses, and contagions like diseases. This is detrimental to human societies in terms of compromised security, monetary loss and life threats. Therefore, to mitigate such damages, identifying and timely quarantining the sources of such diffusion processes is highly critical. Despite the difficulty and challenges of the problem, researchers have extensively studied source identification in complex networks over the past decade. Several approaches have been proposed, but limited attention has been given to the classical graph centrality measures. Moreover, researchers have generally advised against employing these measures for identifying infection sources. Motivated by the same, in this paper, we revisit these measures in context to source identification and raise the question: "Are classical graph centrality measures really not good enough?", and perform an extensive experimental journey. We pick five such measures, viz., betweenness, closeness, degree, eigenvector and eccentricity, and conduct an in-depth analysis of their effectiveness in source detection. Our extensive results show that, contrary to the popular belief, a combination of eccentricity and closeness (EC+CC) generally performs better than several state-of-the-art source identification techniques, with higher accuracy and lower average hop error. We also analyze the impact of infection size on source identification and observe that EC+CC is generally highly scalable and stable as well. We also understand that as the infection size increases, the detection accuracy decreases, irrespective of the technique used. However, when we examine the effect of graph density, we observe that as the graph density increases, the detection accuracy increases as well, with EC+CC again outperforming state-of-the-art. |
| 4. | **A Scalable and Energy-Efficient Concurrent Binary Search Tree with Fatnodes**<br>P Alapati, VK Tavva, M Mutyam - IEEE Transactions on Sustainable Computing, 2020<br><br>**Abstract:** In the recent past, devising algorithms for concurrent data structures has been driven by the need for scalability. Also, there is increased traction across the industry towards power efficient concurrent data structure designs. In this context, we introduce a scalable and energy-efficient concurrent binary search tree with fatnodes (namely, FatCBST), and present algorithms to perform basic operations on it. Unlike a single node with one value, a fatnode consists of a set of values. FatCBST minimizes structural changes while performing update operations on the tree. In addition, fatnodes help to exploit the spatial locality in the cache hierarchy and also reduce the height of the tree. FatCBST allows multiple threads to perform update operations on an existing fatnode simultaneously. Experimental results show that for low contention workloads as well as large set sizes, FatCBST scales well and also provides high performance-per-watt values as compared to the state-of-the-art implementations. For high contention workloads with small set sizes, FatCBST suffers from contention. |
| 5. | **An Unknotting Index for Virtual Knots**<br>S Kamada, K Kaur, A Kawauchi, P Madeti - Tokyo Journal of Mathematics, 2019<br><br>**Abstract:** In this paper we introduce the notion of an unknotting index for virtual knots. We |

| | |
|---|---|
| | give some examples of computation by using writhe invariants, and discuss a relationship between the unknotting index and the virtual knot module. In particular, we show that for any non-negative integer nn there exists a virtual knot whose unknotting index is (1, n). |
| 6. | [Analytical evaluation of damage probability matrices for hill-side RC buildings using different seismic intensity measures](#)<br>M Surana, A Meslem, Y Singh, DH Lang - Engineering Structures, 2020<br><br>**Abstract:** In the present study seismic response and vulnerability of hill-side RC buildings, often observed in the Indian Himalayan region as well as in some other parts of the world were analytically investigated using non-linear dynamic analyses. The conducted analyses led to the development of seismic fragility functions based on three different ground-motion intensity measures, viz. peak ground acceleration, spectral acceleration at the fundamental building period, and average spectral accelerations over a range of periods. In addition to the different code design levels that are considered in the assessment, the choice of the ground-motion intensity measure as well as the structural configuration type of these hill-side buildings show quite significant effects on the resulted damage probabilities of different damage states, and thus on the computed mean damage ratio. The peak ground acceleration results in a significant overestimation of the mean damage ratio for the maximum considered earthquake hazard level when compared with the spectral acceleration-based intensity measures. On the other hand, the irregular structural configuration of hill-side buildings alone results in a significantly higher mean damage ratio when compared with regular structural configuration. In addition to the design code level, the need to incorporate both of these effects, i.e. the choice of ground-motion intensity measure and irregular structural configurations of hill-side buildings, in the next generation of earthquake loss estimation studies and software tools is underlined. |
| 7. | [Automatic Speech-Gesture Mapping and Engagement Evaluation in Human Robot Interaction](#)<br>B Ghosh, A Dhall, E Singla - 28th IEEE International Conference on Robot and Human Interactive Communication, 2019<br><br>**Abstract:** In this paper, we present an end-to-end system for enhancing the effectiveness of non-verbal gestures in human robot interaction. We identify prominently used gestures in performances by TED talk speakers and map them to their corresponding speech context and modulated speech based upon the attention of the listener. Gestures are localised with convolution neural networks based approach. Dominant gestures of TED speakers are used for learning the gesture-to-speech mapping. We evaluated the engagement of the robot with people by conducting a social survey. The effectiveness of the performance was monitored by the robot and it self-improvised its speech pattern on the basis of the attention level of the audience, which was calculated using visual feedback from the camera. The effectiveness of interaction as well as the decisions made during improvisation was further evaluated based on the head-pose detection and an interaction survey. |
| 8. | [Combined influence of fluid viscoelasticity and inertia on forced convection heat transfer from a circular cylinder](#)<br>C Sasmal, MB Khan, RP Chhabra – Journal of Heat Transfer, 2020<br><br>**Abstract:** In this study, the combined influence of fluid viscoelasticity and inertia on the flow and heat transfer characteristics of a circular cylinder in the steady laminar flow regime have been studied numerically. The momentum and energy equations together with an appropriate |

viscoelastic constitutive equation have been solved numerically using the finite volume method over the following ranges of conditions: Reynolds number, 0.1≤Re≤200.1≤Re≤20; elasticity number (= Wi/Re, where Wi is the Weissenberg number), 0≤El≤0.50≤El≤0.5; Prandtl number, 10≤Pr≤10010≤Pr≤100 for Oldroyd-B and finitely extensible nonlinear elastic-Peterlin (FENE-P) (with two values of the chain extensibility parameter L2, namely 10 and 100) viscoelastic fluid models including the limiting case of Newtonian fluids (El = 0). New extensive results are presented and discussed in terms of the streamline and isotherm profiles, drag coefficient, distribution of the local and surface averaged Nusselt number. Within the range of conditions embraced here, the separation of boundary layers (momentum and thermal) is seen to be completely suppressed in an Oldroyd-B fluid whereas it is accelerated for a FENE-P fluid in comparison with that seen for a Newtonian fluid otherwise under identical conditions. At a fixed elasticity number, both the drag coefficient and average Nusselt number are seen to be independent of the Reynolds number beyond a critical value for an Oldroyd-B fluid. In contrast, the drag coefficient decreases and the average Nusselt number increases with Reynolds number for a FENE-P fluid at a constant value of the elasticity number. Finally, a simple correlation for the average Nusselt number for a FENE-P fluid is presented which facilitates the interpolation of the present results for the intermediate values of the governing parameters and/or its a priori estimation in a new application.

---

9.

Directional dependent variation in mechanical properties of planar anisotropic porcine skin tissue
P Lakhani, KK Dwivedi, N Kumar - Journal of the Mechanical Behavior of Biomedical Materials, 2020

**Abstract:** Nonlinear and anisotropic mechanical behavior of skin is essential in various applications such as dermatology, cosmetic products, forensic science, and computational studies. The present study quantifies the mechanical anisotropy of skin using the bulge method and full-field imaging technique. In bulging, the saline solution at 37 °C mimics the in vivo body temperature and fluid conditions, and all experiments were performed in the control environment. Assumption of thin spherical shell membrane theory and imaging techniques were implemented to obtain the anisotropic stress strain relations. Further, stress strain relations at an interval of 10° were calculated to obtain the variation in modulus with direction. Histological examinations were performed to signify the role of the collagen fibers orientation on the mechanical properties. The maximum and minimum linear modulus and collagen fiber orientation intensity were found in good agreement. The angular difference between maximum and minimum linear modulus and orientation intensity was found 71° ± 7° and 76° ± 5° respectively, and the percentage difference was 43.4 ± 8.2 and 52.5 ± 6.4 respectively. Further, a significant difference in the maximum and minimum collagen orientation intensity between the untested and tested specimens indicates the realignment of the fibers. Additionally, a cubic polynomial empirical relation was established to calculate the quantitative variation in the apparent modulus with the directions, which serves for the anisotropic modeling of the skin. The experimental technique used in this study can be applied for anisotropic quantification of planar soft tissues as well as can be utilized to imitate the tissue expansion procedure used in reconstructive surgery.

| | |
|---|---|
| 10. | [Drivers of brand credibility in consumer evaluation of global brands and domestic brands in an emerging market context](#)<br>A Srivastava, DK Dey, MS Balaji - Journal of Product & Brand Management, 2020<br><br>**Abstract:**<br>Purpose<br>The purpose of this study is to examine the impact of brand credibility on purchase intentions toward global brands and domestic brands in an emerging market context. It further examines three drivers of brand credibility: perceived globalness, perceived local iconness and perceived authenticity.<br>Design/methodology/approach<br>A structured questionnaire was used for data collection. Systematic random sampling using the mall intercept technique was used to collect cross-sectional data from 836 customers in India. Hypotheses were tested by using structural equation modeling with AMOS 21.<br>Findings<br>The results demonstrate the significance of brand credibility on purchase intentions. Furthermore, brand globalness differentially influence brand credibility for global and domestic brands.<br>Research limitations/implications<br>The findings provide key insights for marketers regarding consumer evaluation of global brands and domestic brands in emerging markets.<br>Originality/value<br>This study contributes to the literature by proposing and testing the key role of brand credibility in consumer choice of global brands versus domestic brands in an emerging market context. |
| 11. | [Effect of increase in Nano-particle Addition on Mechanical and Microstructural Behaviour of HVOF and Cold-Spray Ni-20Cr Coatings on Boiler Steels](#)<br>M Kumar, H Singh, N Singh - Materials Today: Proceedings, 2020<br><br>**Abstract:** In the present work, Micron and nano-sized powders of Ni and Cr were blended in various proportions by mechanical milling, maintaining Ni (wt.% 80) and Cr (wt.% 20) as the overall weight %, to produce three different grain sized Ni-Cr nano-crystalline alloy powders. These in-house prepared nanocrystalline powders were sprayed on chosen SA 516 boiler steels in this study, using high-velocity oxy-fuel (HVOF) and cold spray (CS) processes. All the deposited coatings were found to have the nano-sized grains. Further the effect of different weight percentages of nano-particles on the microhardness and scratch resistance of coatings was studied. It was concluded that on enhancement in weight % nano-particle, the microhardness of the coatings enhanced. The maximum hardness was found to be 525 Hv and 601 Hv respectively for HVOF and CS coatings. XRD analysis was used to identify phases, SEM/EDS for microstructure analysis and X-ray mapping for elemental distribution in case of all the developed coatings. |
| 12. | [Effect of ground heat extraction on stability and thermal performance of solar ponds considering imperfect heat transfer](#)<br>S Verma, R Das - Solar Energy, 2020<br><br>**Abstract:** This work revisits the idea of ground heat extraction in solar ponds by addressing various limitations associated with the conventional assumption of perfect heat transfer. For this, |

| | |
|---|---|
| | an overall heat transfer coefficient, $U$ has been introduced to analyse the heat extraction taking place from the ground beneath the pond. The pond's thermal performance is analysed for different values of $U$ using closed form solutions and significant departure is seen with respect to the conventional assumption of an infinite $U$. Temperature distributions across various zones are obtained which exhibit deviation from the ideal distributions. It is also observed that the optimum size of non-convective zone yielding maximum efficiency depends on the effectiveness of ground heat extraction. Further, calculations are made for the minimum salt diffusion rate required to sustain stable pond operation. It is observed that the idealized exchanger performance assumption underestimates this critical value and a design based on it may initiate instability. Finally, calculations are made for the net entropy production rate which is also seen to be under-predicted with the existing theory. The present work can therefore prove useful for making an accurate assessment of the performance and stability of solar ponds involving ground heat extraction. |
| 13. | Enhanced adsorption sites in monolayer MoS2 pyramid structures for highly sensitive and fast hydrogen sensor<br>AV Agrawal, R Kumar, G Yang, J Bao, M Kumar, M Kumar - International Journal of Hydrogen Energy, 2020<br><br>**Abstract:** Here, we present a highly sensitive and fast hydrogen ($H_2$) sensor for 1% $H_2$, well below the critical limit of explosion ignite in air, in a temperature range of 28–150 °C by using monolayer $MoS_2$ pyramid structures with enhanced adsorption sites. The monolayer $MoS_2$ pyramid structures is synthesized by modified chemical vapor deposition technique and characterized by field emission scanning electron microscopy, Raman, photoluminescence and atomic force microscopy. The highest sensitivity of 69.1% was achieved at a moderate temperature with a response time of 32.9 s for the monolayer $MoS_2$ pyramid structures. At room temperature (RT), the sensor showed a sensitivity of 6% with a faster response of 11.3 s and recovery time of 125.3 s. The availability of favourable adsorption sites on in-plane $MoS_2$ and edges of $MoS_2$ in monolayer $MoS_2$ structures provide enhanced adsorption sites for gas sensing and resulted in the high sensitivity and low response time compared to that of bare $MoS_2$ and other nanostructures-based $H_2$ sensor. The detailed gas sensing mechanism is proposed in the light of detail surface morphology and density function theory (DFT). This study reveals that tailoring the favourable adsorption sites in 2D materials is helpful to develop the highly sensitive and fast $H_2$ sensor for next generation safety devices for $H_2$ fueled vehicle and clean energy applications. |
| 14. | Enhanced visible-light-assisted photocatalytic hydrogen generation by MoS2/g-C3N4 nanocomposites<br>CM Nagaraja, M Kaur, S Dhingra - International Journal of Hydrogen Energy, 2020<br><br>**Abstract:** A facile, one-pot, solvothermal synthesis of MoS2 microflowers (S1) and the heterostructures MoS2/g-C3N4 with varying ratios of 1:1 (S2), 1:2 (S3) and 1:3 (S4) exhibiting enhanced visible-light-assisted H2 generation by water splitting has been reported. The compounds were thoroughly characterized by PXRD, FESEM, HRTEM, EDS, UV–vis and XPS techniques. FESEM and HRTEM analyses showed the presence of microflowers composed of nano-sized petals in case of pure MoS2 (S1), while the MoS2 microflowers covered with g-C3N4 nanosheets in case of MoS2/g-C3N4 heterostructure, S4. XPS analysis of S2 showed the presence of 2H phase of MoS2 with g-C3N4. The Eosin-Y/dye-sensitized visible-light-assisted |

photocatalytic investigation of the samples in the absence of any noble metal co-catalyst revealed very good water splitting activity of MoS2/g-C3N4 heterostructure, S2 with hydrogen generation rate of 1787 μmol h−1g−1 which is about 6 and 40 times higher than pure MoS2 and g-C3N4 respectively. The relatively higher catalytic activity of the heterostructure, S2 has been ascribed to the efficient spatial separation of photo-induced charge carriers owing to the synergistic interaction between MoS2 and g-C3N4. A possible mechanism for the Eosin-Y-sensitized photocatalytic H2 generation activity of MoS2/g-C3N4 heterostructures has also been presented. The enhanced activity of S2 was further supported by fluorescence measurements. Thus, the present study highlights the importance of non-noble metal based MoS2/g-C3N4 heterojunction photocatalysts for efficient visible-light-driven H2 production from water splitting.

**Graphical Abstract:** A facile solvothermal synthesis of MoS2 nanosheets (S1) and MoS2/g-C3N4 heterostructures with varying ratios of 1:1 (S2), 1:2 (S3) and 1:3 (S4) is reported. The visible light assisted photocatalytic investigation of the samples in the absence of noble metal co-catalyst revealed very good water splitting activity of the heterostructure, S2 with hydrogen generation rate of 1787 μmolh−1g−1, which is found to be higher than those of pure MoS2 and g-C3N4 compounds. The relatively higher catalytic activity of S2 has been attributed to the synergistic effect of MoS2 and g-C3N4 and the presence of highly reactive edge sites of MoS2. Furthermore, the plausible mechanism for the formation of MoS2 nanosheets and MoS2/g-C3N4 heterostructures along with their water splitting activity has been presented.
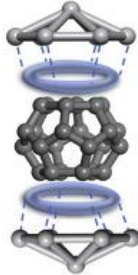


---

15.
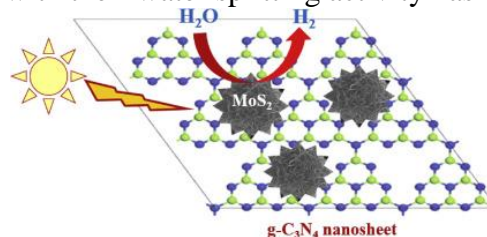
[Exploiting Redundancy and Mobility in Energy-Efficient Communication for WBANs](#)
A Vyas, S Pal - Proceedings of the 21st International Conference on Distributed Computing and Networking, 2020

**Abstract:** Sensor nodes attached with the human body continuously sense and transfer real-time raw data to the coordinator node. The continuous process of sensing generally produces redundant data, which drains energy of the nodes. We study real medical dataset of diabetes, heart rate and body temperature to analyze redundancy in sensed data. We also collected and studied the human pulse rate of different subjects gathered by using pulse sensor for the duration of 20 minutes. This study confirms that redundancy is present in all datasets. Therefore, we propose an auto-regression based prediction algorithm to decide the minimum sampling frequency (rate with which node will sense data) of sensor nodes. This sampling frequency could provide reliable medical information with tolerable prediction error. Additionally, the line-of-sight of communications (LOS) also plays a significant role in the energy consumption of the network. We design Scenario 1 (human standing) and Scenario 2 (walking posture) to study the effect of LOS on the lifetime of the network. In order to address the non-LOS communication, we propose an opportunistic communication protocol for intra-WBANs. The protocol exploits human mobility and data redundancy to maximize the lifetime of the network. Our proposed

| | |
|---|---|
| | approach ensures that the remaining lifetime of the nodes is higher compared to other existing relay-based intra-WBAN communication protocols, such as SIMPLE and ATTEMPT. The proposed method is also having least pathloss effect compared to other protocols. |
| 16. | Generating autofocused aberration laser beams with different spectral performance<br>SN Khonina, V Pal - Journal of Optics, 2020<br><br>**Abstract:** We present a flexible approach for generating autofocused aberration laser beams (ALBs) of different wavelengths based on the diffractive optical element (DOE) design with distinct phase transmittance that has radial power q and periodic angular dependence $\sin(m\varphi)$. The diffraction pattern of ALBs strongly depends on the periodic angular power controlled phase of the DOE. During free-space propagation, the ALBs with different wavelengths convert into different light distributions that have mth-order symmetry (for odd m) and 2mth-order symmetry (for even m). The ALBs exhibit autofocusing properties that significantly differ at longer wavelengths relatively with smaller wavelengths. The formation of light intensity distributions in free-space propagation has a sharp focusing feature that strongly depends on the radial power q. The numerically simulated results are presented for wavelengths in the infrared, visible, and ultra-violet regimes. The experimental findings measured at a wavelength of $\lambda = 1064$ nm, show good agreement with the numerically simulated results and thus verifying our approach. |
| 17 | Hydrogen storage capacity of low-lying isomer of C24 functionalized with Ti<br>RY Sathe, H Bae, H Lee, TJD Kumar - International Journal of Hydrogen Energy, 2020<br><br>**Abstract:** Hydrogen energy is a sustainable and eco-friendly substitute for reducing fossil fuel dependency and boost the air quality index. High-density reversible hydrogen storage as a vehicular fuel is the biggest challenge. Hydrogen storage capacity in Jahn-Teller distorted C24 fullerene functionalized with Ti is studied by using density functional theory. It is found that Ti atoms form two hexagonal pyramidal clusters due to high cohesive energy. Four hydrogen molecules are adsorbed by each Ti through Kubas interaction with adsorption energies in the range of 0.33–0.76 eV/$H_2$. Our findings of practical hydrogen storage capacity and the van 't Hoff desorption temperature reveal that hydrogen molecules are reversibly stored under operable thermodynamic conditions with 10.5 hydrogen weight %. Storage parameters meet the US Department of Energy targets making it a prospective hydrogen storage material.<br><br>**Graphical Abstract:**<br><br> |
| 18. | Impedance spectroscopy of polyvinyl alcohol-coated carboxyl-functionalized single-walled carbon nanotube flexible film: a generic battery model<br>S Meikap, AK Das, AK Meikap - Journal of Materials Science: Materials in Electronics, 2020<br><br>**Abstract:** In this study, we demonstrate a simple technique to prepare a flexible single-walled |

| | |
|---|---|
| | carbon nanotube (SWCNT) array for battery application. The polyvinyl alcohol-coated unidirectional SWCNT flexible film has been prepared using a simple solution casting technique. The frequency variation of impedance spectroscopy of the composite film is investigated in a frequency spectrum of $20\,\text{Hz} \le f \le 1\,\text{MHz}$ and temperature range $(373 \le T \le 413\,\text{K})$. The experimental data are simulated with a generic battery model equivalent circuit. The generalized model is based on impedance spectroscopy, which is suitable for practical application and able to interpret the existing battery model. The extracted parameters from the simulation of experimental data are tabulated. The temperature variation of the parameters is very significant for manufacturing a battery system. The study of electric modulus suggests a non-Debye-type relaxation behavior of the flexible battery system. |
| 19. | Improved performance of a nanorefrigerant-based vapor compression refrigeration system: A new alternative<br>L Kundan, K Singh - Proceedings of the Institution of Mechanical Engineers, Part A, 2020<br><br>**Abstract:** An attempt has been made to improve the heat transfer characteristics of the vapor compression refrigeration cycle using nanorefrigerant (R134a and $Al_2O_3$, size $20\,\text{nm}$). The performance parameters such as, coefficient of performance, cooling capacity, energy consumption, and temperature drop across condenser and evaporator have been investigated and analyzed. This has been done by varying the mass fraction of nanoparticles of $Al_2O_3$ (0.5–1 wt%) and the flow rate of nanorefrigerant. The investigation has been carried out using three types of nanorefrigerants, i.e. pure R134a, R134a+$Al_2O_3$ (0.5 wt%), and R134a+$Al_2O_3$ (1 wt%) at flow rates of $6.5\,\text{L/h}$ and $11\,\text{L/h}$, respectively. The coefficient of performance of the refrigeration system using 0.5% of $Al_2O_3$ (wt%) is found to be improving with volume flow rates of nanorefrigerant, i.e. 7.20% for $6.5\,\text{L/h}$ and 16.34% for $11\,\text{L/h}$. The use of nanorefrigerant (R134a+$Al_2O_3$) has also resulted in a significant increase in the cooling capacity of the refrigeration system. A substantial drop in the temperature across the condenser (3.0–23.77%), and gain in temperature across the evaporator (4.69–39.30%) is also observed for the refrigeration system under investigation. |
| 20. | Interfacial study of vertically aligned n-type MoS2 flakes heterojunction with p-type Cu-Zn-Sn-S for self-powered, fast and high performance broadband photodetector<br>AV Agrawal, K Kaur, M Kumar - Applied Surface Science, 2020<br><br>**Abstract:** The p-n junction is an influential trait for efficient charge transport in electronic and optoelectronic devices. Demonstrating p-n junction using 2D TMDCs is inescapable to integrate these materials with matured 3D material technology, as 2D material offers easy integration due to the absence of dangling bonds. However, understanding the electronic properties at the interface is crucial for rational design of heterojunction devices for their novel and unmatched functionality. Present work reports detail interfacial study and band-alignment of two potential materials, 3D $Cu_2ZnSnS_4$(CZTS) and 2D-layered $MoS_2$. The detail photoelectron spectroscopy measured the valance band offset (VBO) and conduction band offset (CBO) of $-0.23 \pm 0.1\,\text{eV}$ and $-0.29 \pm 0.1\,\text{eV}$, respectively and established a favorable type-II band-alignment at CZTS/$MoS_2$ interface. Significant PL quenching at CZTS/$MoS_2$ interface proven to be strong evidence of efficient charge transport. As a proof of concept, a self-driven CZTS/$MoS_2$ heterojunction broadband photodetector was constructed exhibiting pronounced photovoltaic features with high responsivity $141\,\text{mA/W}$, outstanding photoswitching capability ($I_{On}/I_{Off} = 112$) and fast response ($\tau_r/\tau_d = 81/79\,\text{ms}$). The responsivity was further enhanced to |

79A/W at moderate bias (@6V). Additionally, the device showed exceptional stability after 1500 h of operation. This work intends to trigger the research on 3D/2D for high performing optoelectronic devices based on CZTS/MoS$_2$ heterojunctions.

**Graphical Abstract:** Device Schematic of CZTS/MoS2 p-n heterojunction photodetector with Type II band alignment showing high performance with efficient cyclability in self-driven mode.



---

21.
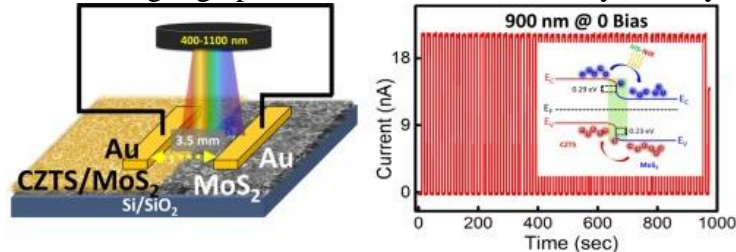
[Inverse Optimization of Design Parameters in a Hybrid Solar Pond System with External Heat Addition](#)
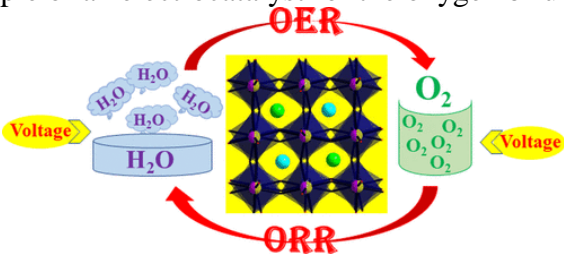A Kumar, R Das - ASME 2019 International Mechanical Engineering Congress and Exposition, 2020

**Abstract:** External heat supply to solar ponds from various types of solar collectors is a feasible alternative that significantly enhances its performance. In this work, various design parameters in a hybrid solar pond with external heat addition from Evacuated Tube Solar Collector (ETSC) are evaluated using an inverse approach. A forward model based on heat balance equations is solved for various zones of the solar pond to predict temperatures attained by its storage zone under a given climatic condition. Bryant and Colbeck's relation is used to account for the diminution of the solar radiation as it travels from upper layers of the solar pond to its bottom layers. The relevant differential equations are solved using a Runge-Kutta fourth order scheme. The component of heat addition from ETSC is added to the forward model in the storage zone's equation. Heat added from ETSC is considered proportional to the fraction of the aperture area to the pond's base area, the thermal efficiency of ETSC and global solar radiation incident on ETSC. Both the forward model of the solar pond and combined solar pond and ETSC model were validated with previous experimental and numerical studies available in the literature for El Paso, USA, and Melbourne, Australia. An inverse model based on genetic algorithm is proposed for evaluating the set of geometrical parameters of ETSC and solar pond in order to derive a required performance from the combined solar pond-ETSC system.

---

22.

[Investigating the temporal dynamics of electroencephalogram (EEG) microstates using recurrent neural networks](#)
A Sikka, H Jamalabadi, M Krylova, S Alizadeh… DR Bathula - Human Brain Mapping, 2020

**Abstract:** Electroencephalogram (EEG) microstates that represent quasi-stable, global neuronal activity are considered as the building blocks of brain dynamics. Therefore, the analysis of microstate sequences is a promising approach to understand fast brain dynamics that underlie various mental processes. Recent studies suggest that EEG microstate sequences are non-Markovian and nonstationary, highlighting the importance of the sequential flow of information between different brain states. These findings inspired us to model these sequences using Recurrent Neural Networks (RNNs) consisting of long-short-term-memory (LSTM) units to capture the complex temporal dependencies. Using an LSTM-based auto encoder framework

and different encoding schemes, we modeled the microstate sequences at multiple time scales (200–2,000 ms) aiming to capture stably recurring microstate patterns within and across subjects. We show that RNNs can learn underlying microstate patterns with high accuracy and that the microstate trajectories are subject invariant at shorter time scales ($\leq$400 ms) and reproducible across sessions. Significant drop in the reconstruction accuracy was observed for longer sequence lengths of 2,000 ms. These findings indirectly corroborate earlier studies which indicated that EEG microstate sequences exhibit long-range dependencies with finite memory content. Furthermore, we find that the latent representations learned by the RNNs are sensitive to external stimulation such as stress while the conventional univariate microstate measures (e.g., occurrence, mean duration, etc.) fail to capture such changes in brain dynamics. While RNNs cannot be configured to identify the specific discriminating patterns, they have the potential for learning the underlying temporal dynamics and are sensitive to sequence aberrations characterized by changes in metal processes. Empowered with the macroscopic understanding of the temporal dynamics that extends beyond short-term interactions, RNNs offer a reliable alternative for exploring system level brain dynamics using EEG microstate sequences.

---

**23.**

[Investigation of New B-Site-Disordered Perovskite Oxide CaLaScRuO6+ δ: An Efficient Oxygen Bifunctional Electrocatalyst in a Highly Alkaline Medium](#)
N Kumar, M Kumar, TC Nagaiah, V Siruguri… - ACS Applied Materials & Interfaces, 2020

**Abstract:** Energy storage and conversion driven by electro- or photocatalyst is a highly exciting field of research, and generations of effective and durable oxide catalysts have received much attention in this field. Here, we report A-site lanthanum-doped oxygen-rich quinary oxide CaLaScRuO6+$\delta$ synthesized by adopting the solid-state reaction method and characterized by various techniques such as powder X-ray diffraction, neutron diffraction, energy-dispersive X-ray spectroscopy, inductively coupled plasma-atomic emission spectrometry, Raman spectroscopy, and temperature-programmed reduction in the presence of a hydrogen atmosphere (H2-TPR). X-ray absorption study confirms the existence of mixed valent Ru ions in the structure, which enhances the oxygen stoichiometry for the partial balance of an extra cationic charge. Neutron powder diffraction and reduction of the material in a hydrogen atmosphere (H2-TPR) can confirm the oxygen overstoichiometry of the catalyst. The present material works as an efficient and robust oxygen bifunctional electrocatalyst for ORR/OER (oxygen evolution reaction/oxygen reduction reaction) followed by four-electron transfer pathway in a strong (1 M KOH) alkaline medium. The catalytic nature of the designed structural and chemical flexible perovskite is a novel example of an electrocatalyst for the oxygen bifunctional activity.

---

**24.**

[Mimicking high strength lightweight novel structures inspired from the trabecular bone microarchitecture](#)
N Kumar, A Kumar, P Uniyal, B Ramalingaiah… - Philosophical Transactions of the Royal Society A, 2020
**Abstract:** Nature's evolution of a billion years has advanced flawless functionality in limitless

optimized structures like bone structural adaptation in various physiological behaviours. In this study, porous structures are designed and fabricated from the nature-inspired trabecular bone microarchitecture. A three-dimensional (3D) model of the porous trabecular architecture from the compressive proximal zone of the femoral head was constructed using the micro-computed tomography scanning tool. The model was modified to get porous structures of different volume fractions varying from 20 to 40% with an increment of 10%. The obtained porous structures were 3D printed and analysed for deformation-resistant behaviour. Quasi-static compressive loading was performed at different strain rates ($0.001–1\ \mathrm{s}^{-1}$) to get an insight into lightweight, high strength structural behaviour. Mechanical parameters, such as specific modulus, specific strength and specific energy absorption, were analysed for the optimal volume fraction. The original volume fraction (30%) of the trabecular bone shows the highest value of mechanical parameters. This study can help engineers to select and design lightweight porous structures with high energy-absorbing capacity, mimicking the desired architecture and porosity available in nature.

This article is part of the theme issue 'Bioinspired materials and surfaces for green science and technology (part 3)'.

| | |
|---|---|
| 25. | Multiparticle production and geometric scaling in 5.44 TeV Xe–Xe collisions at the CERN Large Hadron Collider using wounded quark model <br> OSK Chaturvedi, PK Srivastava, A Singh, PK Raina… - The European Physical Journal Plus, 2020 <br><br> **Abstract:** Recently, CERN Large Hadron Collider has performed a collision experiment of xenon–xenon (Xe–Xe) nuclei at $\sqrt{s}NN=5.44\mathrm{TeV}$. The experiment based on Xe–Xe nuclei can provide a deeper understanding of the particle production mechanism in QCD. In this article, we have studied midrapidity pseudorapidity density ($(dn_{ch}/d\eta)\eta=0$) of charged hadrons with respect to collision centrality using the modified version of wounded quark model (WQM). In WQM, we have constructed minimum-bias event sets in two different ways denoted as Class I and Class II. Further, we have shown the scaling behavior of $(dn_{ch}/d\eta)\eta=0$ with respect to the number of participating quarks, Nq. We observed that Class II results satisfy the experimental data quite well. |
| 26. | N-Centered Radical Directed Remote C–H Bond Functionalization via Hydrogen Atom Transfer <br> G Kumar, S Pradhan, I Chatterjee – Chemistry - An Asian Journal, 2020 <br><br> **Abstract:** The N-centered radical directed remote C−H bond functionalization via hydrogen-atom-transfer at distant sites has developed as an enormous potential tool for the organic synthetic chemists. Unactivated and remote secondary and tertiary, as well as selected primary C−H bonds, can be utilized for functionalization by following these methodologies. The synthesis of the heterocyclic scaffolds provides them extra attention for the modern days′ developments in this field of unactivated remote C−H bonds functionalizations. |
| 27. | Numerical investigation on the effect of different physiological cancerous breast parameters on the output of microwave ablation <br> J Kumar, R Repaka – Journal of Engineering and Science in Medical Diagnostics and Therapy, 2020 <br><br> **Abstract:** Microwave ablation is a newly developed minimally invasive tumour therapy which possesses several advantages over the existing thermal therapies. Despite the several advantages, |

| | |
|---|---|
| | microwave ablation also suffers same disadvantages similar to other thermal therapies like poor control over ablation volume. Sensitivity of different tissue parameters is the key factor to design a microwave ablation protocol. In this work, sensitivity analysis has been conducted to quantify the effect of three cancerous breast parameters, viz., breast composition, tumour location and tumour size, on the efficacy of microwave ablation of breast cancer. Ablation volume has been taken as the indicator of the ablation efficacy during microwave ablation procedure. A Taguchi's design of experimental approach has been utilized to optimize the number of simulations required for the analysis and then analysis of variance (ANOVA) has been performed to predict the most sensitive parameter along with their individual contribution. Finite element approach-based simulations have been performed in a Multiphysics software. Firstly, a grid independent study has been established to optimize the number of mesh elements and to reduce the computational cost. Then, after finding the most optimum grid size, all the simulations have been performed in accordance with the protocol obtained from Taguchi's design of experiment approach and finally statistical analysis software has been used for analysing Taguchi's design. It has been found that, the breast composition to be the most significant factor, with maximum contribution in ablation volume, among three considered factors followed by tumour location and tumour size respectively. |
| 28. | Optimization of Aerodynamic Parameters of an Elliptical-Bladed Savonius Wind Rotor Using Multi-Objective Genetic Algorithms<br>N Alom, R Das, UK Saha - ASME 2019 Gas Turbine India Conference, 2020<br><br>**Abstract:** The Savonius wind rotor, a drag-based machine, despite having lesser efficiency has got several advantages such as low price, easy installation, better starting capability independency to wind direction. In order to enhance the performance of such rotor, several design modifications have been built by changing the geometric parameters such as overlap ratio, aspect ratio, tip speed ratio, number of rotor blades and effect of shaft and end plates. Apart from the various geometric parameters, several rotor blades and augmentation techniques has evolved to improve the performance of the Savonius rotor. This has been achieved by using a host of numerical and experimental methods. In the present investigation, the multi-objective genetic algorithms have been used to optimize the incoming velocity, and the torque and lift coefficient for a novel elliptical-bladed profile for maximizing the rotor power coefficient. The multi-physics solver ANSYS direct optimization technique has been used to implement the genetic algorithms. The results obtained from the genetic algorithms have been compared with the established results under identical conditions. |
| 29. | Revisiting gradient layer heat extraction in solar ponds through a realistic approach<br>S Verma, R Das – Journal of Solar Energy Engineering, 2020<br><br>**Abstract:** In this paper, the concept of heat extraction from the gradient zone (GZ) in solar ponds has been analyzed in a more realistic manner to overcome the drawbacks of previously conducted studies. For this purpose, a net heat transfer coefficient has been invoked to investigate the heat transfer occurring from the GZ to the exchanger installed in this zone, in addition to the storage zone (SZ). Analytical solutions for temperature profiles in the GZ and the corresponding exchanger have been obtained which are further used to investigate various aspects of the thermal performance of the pond. The consideration of realistic heat transfer across the GZ exchanger reveals that the ideal thickness of GZ yielding maximum power output is always under-predicted by the idealized assumption of the literature. Unlike intuitive |

| | |
|---|---|
| | perception, the conventional assumption of an infinite heat transfer coefficient does not affect the pond stability because, for all practical purposes, the critical salt diffusion rate predicted by it is always larger than the actual critical value required for ensuring stable pond operation. However, as expected, the rate of exergy destruction caused by the pond's operation is found to be underestimated by the idealized assumption. This study provides a useful analytical tool to make more realistic predictions on various performance parameters of solar ponds utilizing the heat stored in their GZ. |
| 30. | Stoichiometric influences on ion beam nanopatterning of CoSi binary compound<br>BK Parida, S Sarkar - Vacuum, 2020<br><br>**Abstract:** Impact of initial stoichiometry of binary compound on surface nanostructure formation with low energy ion irradiation has been studied. Different stoichiometric CoSi surfaces are irradiated by $Ar^+$ ion beam with energy of 700 eV, fluence of $7.5\times10^{18}$ ions $cm^{-2}$ and angle of incidence 67°. Within a narrow window of stoichiometric variation, self-organized nanoripples have been observed. The ripple structures are well formed for stoichiometric ratios of 40:60 for Co:Si. Nanoscale ripples start growing for a concentration of about $Co_{22}Si_{78}$. The root mean square (rms) roughness initially decreases and then increases slightly as Co increases from low to medium concentrations. The evolution of different morphologies has been corroborated from the behavior of power spectral densities (PSD). Correlation lengths are extracted from atomic force microscopy (AFM) images to corroborate the ripple formation region only within a specific stoichiometric range. Differential sputtering yields provide a rationale for the observed pattern evolution. |
| 31. | Strange nonchaos in self-excited singing flames<br>D Premraj, SA Pawar, L Kabiraj, RI Sujith - EPL (Europhysics Letters), 2020<br><br>**Abstract:** We report the first experimental evidence of a strange nonchaotic attractor (SNA) in the natural dynamics of a self-excited laboratory-scale system. In the previous experimental studies, the birth of a SNA was observed in quasiperiodically forced systems; however, such evidence of a SNA in an autonomous laboratory system is yet to be reported. We discover the presence of a SNA between the attractors of quasiperiodicity and chaos through a fractalization route in a laboratory thermoacoustic system. The observed dynamical transitions from order to chaos via a SNA is confirmed through various nonlinear characterization methods prescribed for the detection of a SNA. |
| 32. | The Effect of Strain Rate on the Stress Relaxation of the Pig Dermis: 2 A Hyper-Viscoelastic Approach 3<br>KK Dwivedi, P Lakhani, S Kumar, N Kumar - Journal of Biomechanical Engineering, 2020<br><br>**Abstract:** The understanding of strain rate dependent mechanical properties of the skin are important for accurate prediction of its biomechanics under different loading conditions. The present study investigated the effect of strain rate i.e. 0.025/s (low), 0.5/s (medium) and 1.25/s (high), ranging in the physiological loading rate of connective tissue, on the stress relaxation response of the porcine dermis. Results show that in the initial phase of the relaxation, the value of stress relaxation (extent of relaxation) was found higher for high strain rate, whereas the equilibrium stress was found strain rate independent. A Mooney-Rivlin based five-term quasilinear viscoelastic model was proposed to determine the effect of strain-rate on the stress relaxation behavior of the porcine dermis. The value of relaxation modulus G1 and G2 were |

| | |
|---|---|
| | found higher for the high strain rate, whereas the reverse trend was observed for G3, G4, and G5. Further, the value of time constants t1, t2, t3, t4 and t5 were found higher for low strain rate. statistical analysis shows no significant difference in the values of G5, t4 and t5 among the three strain rates. The proposed model was found capable to fit the stress relaxation response of skin with great accuracy with RMSE value equal to $0.015 \pm 0.00012$ MPa. Moreover, this hyper-viscoelastic model can be utilized; to quantify the effect of age and diseases on the skin to simulate the stresses on sutures during large wound closure and impact loading. |
| 33. | ZIF-8-Nanocrystalline Zirconosilicate Integrated Porous Material for the Activation and Utilization of CO2 in the Insertion Reactions<br>D Srivastava, P Rani, R Srivastava - Chemistry–An Asian Journal, 2020<br><br>**Abstract:** The conversion of CO2 to useful chemicals, especially to atom economical products, is the best approach to utilize an excess of CO2 present in the atmosphere. In this study, a metal-organic framework ZIF-8 is integrated with nanocrystalline zirconosilicate zeolite to develop an integrated porous catalyst for the CO2 insertion reactions. The catalyst exhibits excellent activity for the CO2 insertion reaction of epoxide to produce cyclic carbonate in neat condition without the addition of any co-catalyst. The catalyst is stable and recyclable during the cyclic carbonate synthesis. Further, the catalyst also exhibits very good activity in another CO2 insertion reaction to produce quinazoline-2,4(1H, 3H)-dione. |